Research Square

Preprints are preliminary reports that have not undergone peer review.
They should not be considered conclusive, used to inform clinical practice,
or referenced by the media as validated information.

Climate and urban form explain shade patterns in U.S. cities

V. Kelly Turner

vkturner@ucla.edu

University of California Los Angeles, California, USA

Isaac Buo

Arizona State University

Ariane Middel

Arizona State University https://orcid.org/0000-0002-1565-095X

Jean Claude Iradukunda

University of California Los Angeles

Article

Keywords: Heat, Cities, Trees, Local Climate Zones, Köppen climate classifications

Posted Date: August 3rd, 2026

DOI: https://doi.org/10.21203/rs.3.rs-10298361/v1

License: This work is licensed under a Creative Commons Attribution 4.0 International License.
Read Full License

Additional Declarations: There is **NO** Competing Interest.

Abstract

Cities lack systematically measured shade data to guide heat planning, even though shade is more effective at reducing radiant heat load than greening and high-albedo surfaces, interventions for which data is widespread. Here, we treat shade as a measurable environmental service shaped by land-systems characteristics, analogous to how land systems science treats NDVI or albedo. Drawing from a national-scale, 1m resolution shade analysis across 330 + U.S. cities, analyzed at the census block group scale at 12:00 h, 15:00 h, and 18:00 h, we find that climate sets the floor for shade by constraining vegetative potential, and urban form sets the ceiling through building shade that dominates late-day shade production. Shade disparities are greatest at noon, but equalize later in the day as building shade increases. These predictable, generalizable patterns position shade for integration into land systems models and heat planning frameworks alongside temperature-based metrics.

1. Introduction

Shade is essential infrastructure for keeping cities livable in a hotter future. Heat is already widely recognized as a leading climate-related public health crisis because it threatens human *survivability* under extreme conditions. Yet, heat also undermines *livability* under more common, moderately hot conditions, when personal heat exposure renders routine daily activities unsafe (Vanos et al. 2023). Personal heat exposure is fundamentally a process of energy transfer to the human body. Outdoors, solar radiation (sunlight) is the primary modifiable source of heat gain, and often the largest additional load under warm conditions (Jay et al. 2021). Shade interrupts that process, enabling people to remain safely active outdoors for longer periods of time and at higher temperatures before reaching “uncompensable” heat stress: the point at which the human body can no longer effectively cool itself (Vanos et al. 2023). This ability to slow the rate of heating and delay critical thermophysiological thresholds makes shade especially effective compared to other outdoor cooling interventions.

For decades, climate science has generated large-scale, high-resolution, accessible data on air and land surface temperatures, supporting a body of research largely focused on urban-rural temperature differences, referred to as the Urban Heat Island effect (Stewart et al. 2011). This data and framing make it relatively easy for local governments to use UHI as a benchmark for cooling, despite known conceptual limitations (Martilli et al. 2020). Surface and air temperature data sets quantify background environmental conditions but do not capture radiant heat, the most salient temperature metric for measuring solar exposure relevant to human heat gain (Middel and Krayenhoff 2019). Variables such as Mean Radiant Temperature (MRT), which capture radiant heat, currently require sophisticated, computationally intensive modeling methods that can limit their regular use in local policy and planning (Schneider et al. 2024). As scholars work toward automating methods for modeling radiant heat exposure (AlKhaled et al. 2024), governments lack a systematically measured and mapped dataset to assess it or integrate targets into policy and plans.

This gap in the ability to use shade or radiant heat to guide local heat planning has negative consequences for heat-health management. In practice, cities have prioritized interventions that align with air and surface temperature variables that are already integrated into decision-support systems. These variables align with outdoor cooling strategies such as urban greening and high-albedo surfaces that produce only modest benefits to human health through ~ 1°C reductions in air temperature and primarily act on surfaces (Wong et al. 2021). Shade, by contrast, directly reduces radiant heat load from solar exposure and can lower MRT by tens of degrees (Middel and Krayenhoff 2019, Middel 2021). The resulting reduction in physiological heat stress is far greater under shade cast by any green or engineered physical element of the environment than through greening or high-albedo surface treatments (Middel 2021). In the absence of reliable, scalable metrics to quantify shade, cities lack the capacity to plan for its intentional delivery, leaving substantial potential to reduce heat exposure unrealized.

While the cooling benefits of shade are delivered directly to individuals where shadows are cast, “shade infrastructure”--the combined set of green and gray physical features that block or filter direct sunlight from reaching people and surfaces, and the institutions that support delivery on developed lands (Turner et al. 2023)--describes broader patterns that shape when and where those benefits are delivered. At local scales, the amount of shade depends on the composition and arrangement of vertical elements such as buildings and vegetation, as well as solar geometry at different times of day or seasons of the year (Middel et al. 2014, Chen et al. 2025). At regional scales, heterogeneity in shade patterns across and among urban regions with different urban morphology has been detected (Zhou et al. 2009, Alexandrowicz 2022, Buo et al. 2023). Separately, at regional scales, it is also well established that climatic regimes constrain vegetative potential and, by extension, the feasibility of vegetation-based shade in water-limited environments (e.g., Roebroek et al. 2025, Nitschke et al. 2017). What is not fully established is whether and how shade infrastructure varies systematically across regions in relation to urban form patterns and climate systems. In the absence of systematic, cross-regional evidence, shade infrastructure is difficult to integrate into scientific and planning frameworks that rely on generalizable, spatially comparable metrics, with the same rigor as urban greening or albedo.

Here, we position shade as an environmental service that can be measured at scale and generalized as a land-system outcome shaped by the characteristics that govern its delivery. This framing supports a conceptual advancement in which shade is treated as a comparable environmental service, with properties that can be systematically characterized across land and climate contexts, on par with urban greening or high-albedo materials. Drawing insight from site and regional-scale shade studies, we focus on two key explanatory variables, urban form and climate, to explain urban shade infrastructure based on their impacts on built features and vegetation. Specifically, we hypothesize that urban form determines the distribution of shade infrastructure and timing of its delivery, while climate constrains the mix of shade-casting features that can be sustained. We further hypothesize that total shade infrastructure is structured by urban form within the constraints imposed by regional climate.

To test these hypotheses, we draw from a high-resolution (1m), national-scale shade map encompassing more than 330 U.S. cities. We conduct a comparative analysis of shade delivery attributes–total shade, vegetation versus built shade, and shade at noon (minimum), 3 pm, and 6 pm (maximum)–at the census block group scale. We relate these shade attributes to urban form and climate using Local Climate Zones and Köppen climate classifications as indicators (Stewart and Oke 2012, Peel et al 2007). Data are analyzed at the Census Block Groups (CBGs) scale to compare patterns in the amount, type (built versus vegetative), and diurnal delivery of shade.

2. Results

2.1 Shade availability varies across and within cities over the diurnal cycle

Shade availability varies widely across and within U.S. cities over the course of a day (Fig. 1). Within cities, minimum CBG total shade at noon ranges from less than 1% to more than 50% across cities, indicating substantial differences in baseline shade availability during peak solar exposure. By 18:00 h, CBG shade could exceed 95%, indicating large differences in the maximum shading capacity. Cities also differ in how shade changes over the diurnal cycle. Some have relatively stable shade availability, with modest (less than 10%) differences between 12:00 and 18:00 h. While others experience large diurnal increases, exceeding baseline shade by more than 2x at maximum capacity. Of the stable shade cities, some remain consistently low-shade (less than 15%) throughout the day, whereas others maintain high shade (above 70%) coverage.

Within all cities, median CBG total shade increases from approximately 25% at 12:00 h to 60% by late afternoon. At 12:00 h, nearly all total shade is vegetative (98%), but by 18:00 h, building shade increases substantially. Nearly all of this diurnal increase (99%) is attributable to building shade as solar angles shift, producing longer building shadows later in the day. By contrast, vegetative shade remains comparatively stable across time, with tree canopy providing a consistent shade footprint throughout the day. From 12:00 to 18:00 h, increases in total shade are strongly associated with increases in building shade ($r = 0.93$), indicating that urban form plays a dominant role in shaping late-day shade capacity.

Within cities, shade availability also varies substantially across CBGs. The range of unevenness is highest at 12:00 h, where the median Gini index is 0.13, meaning that midday shade heterogeneity varies a lot between cities. By 18:00 h, the median Gini index drops mean shade disparity drops (0.08), meaning shade heterogeneity varies less between cities later in the day. The magnitude of shade disparity differs by city. In cities with the largest disparity in shade availability, the difference between the most and least shady CBGs can exceed 80% at all times of the day. Cities with the least disparity have a difference of less than 20% in shade availability between the most and least shady CBGs only at 12:00 h.

2.2 Climate region sets the floor for shade, urban form sets the ceiling

Köppen climate classifications (Fig. 2) explain substantial variation in midday shade across CBGs, primarily through differences in vegetative shade. Arid and semi-arid regions (*BWh*, *BSh*, *BSk*) have the lowest median shade at 12:00 h, typically 15–20%, almost all of which is produced by vegetation (median shade for *BWh*, *BSh*, and *BSk* is 16%,18%, and 21%, respectively). Vegetation shade increases across temperate dry-summer (*Csa*, *Csb*), temperate no-dry-season (*Cfa*, *Dfa*), and cold-summer (*Dsc*, *Dsb*) climates, with median values approaching 30% in several categories (median shade for *Csa*, *Csb*, *Cfa*, and *Dfa* is 22%, 31%, 32%, and 31%, respectively). Tropical rainforest climates (*Af*) exhibit relatively high vegetation shade but do not exceed the highest temperate or cold-summer classes in this dataset. Building shade shows relatively little variation across climate regions and remains a small contributor at midday (less than 1%). These patterns indicate that climate places an upper limit on the extent of vegetative shade, effectively defining minimum shade availability across U.S. cities.

Urban form (Fig. 3) determines the potential for additional shade beyond any climate baseline. Building shade at midday is low across all Local Climate Zones (LCZs), but differences emerge later in the day and could account for more than 90% of total shade in any given CBG. Most CBGs fall within open lowrise LCZs, which account for more than 80% of the sample and produce among the lowest amounts of building shade at 18:00 h (median building shade is less than 20%). Large lowrise areas exhibit building shade levels similar to open lowrise areas across all times of day and tend to have lower vegetative shade (median vegetation shade around 20%). Compact high-rise areas produce the most building shade at 18:00 h (76%), but these areas are rare in the dataset (~ 1%) and show wide variability in building shade (minimum building shade of 2%, maximum building shade of 99%) and tend to have the lowest vegetation shade (median vegetation shade less than 14%). Compact midrise, open highrise, and compact lowrise areas provide moderate (roughly 70%) shade at 18:00 h. These patterns indicate that building height and, in some instances, compactness, define potential additional building shade beyond the baseline established by climate by virtue of vegetation.

Table 1 presents the results for the Type I two-way ANOVA test conducted on the dataset to evaluate the influence of regional and urban climate types on shading coverages. The results indicate that both variables (KPG and LCZ) influence shade coverage at both times with statistical significance (P_value < 0.001). The regional climate variable, KPG has a dominant influence on the shade coverage at both times compared to the local climate variable (LCZ), as suggested by the sums of squares and the F_values. Furthermore, the interaction effect between the two variables (C(KPG):C(KPG)) at solar noon (F_value = 15.48) is more than twice as high as that observed during maximum shade conditions at 18:00 (F_value = 6.72).

Table 1. Two-way ANOVA results for the effect of KPG and LCZ on shading at 12: 00 and 18: 00

Time	Variable	DF	Sum_sq	Mean_sq	F_value	P_value
Shade (12 PM)	C(KPG)	7.0	1.28×10^6	1.83×10^5	1,341.49	0.0
	C(LCZ)	6.0	1.45×10^5	2.41×10^4	176.96	0.0
	C(KPG) :C(LCZ)	42.0	8.87×10^4	2.11×10^3	15.48	0.0
	Residual	30,779.00	4.20×10^6	1.36×10^2	-	-
Shade (6 PM)	C(KPG)	7.0	1.02×10^6	1.46×10^5	615.09	0.0
	C(LCZ)	6.0	3.89×10^5	6.48×10^4	272.51	0.0
	C(KPG) :C(LCZ)	42.0	6.71×10^4	1.60×10^3	6.72	0.0
	Residual	30,779.0	7.32×10^6	2.38×10^2	-	-

Figure 4 shows how maximum shade coverage at 18:00 h varies across urban form and across climate regimes. Across all climate zones, the ranking of LCZs is similar. Compact high-rise and dense trees have the highest shade potential, followed by compact midrise and open high-rise, with the lowest shade potential in open lowrise and large lowrise. This suggests that urban form structures shade potential, regardless of climate, but climate raises or lowers the baseline conditions for shade.

The role of form, establishing the shade ceiling, and climate, strongly influencing the shade floor, is reinforced in Fig. 4b, which shows how much shade is possible at 18:00 h during peak shade production for each LCZ-Köppen pairing. The ordering of shade potential for LCZ and climate baselines remains consistent to the trends in Fig. 4b. Figure 4a describes the shade floor across LCZ-Köppen pairings, and while differences between LCZs are less pronounced at 12:00 h, form still generates differences in shade. Of all LCZs, only dense trees remain consistently high shade producers midday, highlighting the role of trees in producing consistent shade across the diurnal cycle. Compact high-rise, the other large shade producer late in the day, provides far less shade across climate conditions midday.

3. Discussion and conclusion

Our analysis provides the first national-scale, cross-regional evidence that shade infrastructure can be systematically assessed and characterized as an environmental outcome patterned by land characteristics. Urban climate science has established that shade patterns at individual sites result from local permutations of urban form, vegetation, and sun angle (Middel et al. 2021). Computational approaches have enabled scaling of shade mapping to regional and national extents (Zhou et al. 2009,

Alexandrowicz 2022, Buo et al. 2023). Our study builds on these computational advances, revealing that shade patterns are not merely idiosyncratic to specific sites. Instead, climate and urban form interact to create predictable patterns in the magnitude, composition, and timing of shade production across census blocks in 330 U.S. cities.

Specifically, we found that climate establishes the floor for vegetative shade that can be sustained in a region, and urban form sets the ceiling for how much additional shade can be produced from engineered structures, while solar geometry determines when shade from different climate-form combinations is cast. As we expected, climate is a key factor in differentiating vegetation availability (e.g., Roebroek et al. 2025, Nitschke et al. 2017). We found that cities in arid climates begin with structurally lower vegetative shade baselines. Also, as expected, we found that engineered features in the environment contributed distinctly to shade availability over the course of the day (Middel et al. 2014, Chen et al. 2025). Compact and higher-rise areas provided substantial late-afternoon shade, although midday shading was limited. This finding builds on the observation that urban cores tend to produce more shade from buildings, while suburbs derive more shade from trees (Saud and Richter 2026). Urban core sites likely produce more shade from buildings due to larger concentrations of compact and high-rise LCZs. The decline in shade disparity later in the day suggests that building shade can equalize access spatially, but only at specific times. This finding underscores the importance of accounting for both timing and the mechanism of delivery in assessments. These, along with the overall finding that shade exhibits regular and predictable patterns, set the stage to generalize about its causes, consequences, and connect to environmental theory broadly.

In this study, we connected shade to land systems science, a research tradition that treats land composition and configuration as drivers of environmental services, often using data derived from remote sensing at large spatial extents (Dong et al. 2019). This tradition has relied heavily on surface-based observations of state variables such as NDVI and albedo, which characterize horizontal land cover. These variables are linked to thermal states such as LST and air temperature, and the associated Urban Heat Island index (Turner et al. 2022; Li et al., 2023). This omission is consequential because blocking incoming shortwave radiation is among the most metabolically significant determinants of human heat exposure (Middel et al. 2016, Vanos et al. 2023). By conceptualizing shade as a land-systems outcome, we introduce a pathway for integrating vertical structure, shade, and thermal state variables (e.g., MRT) with salience to human health in land systems science frameworks. This path holds promise for bridging the existing gap between surface-based assessments of temperature used in land systems science and site-level understanding of heat exposure in urban climate and public health research.

Incorporating shade into land systems models also improves the ability of planning, policy, and public health practitioners to target radiant heat exposure directly. Most municipalities consume whatever heat-related data products, largely air temperature and surface temperature products, are available to them to direct resources to heat-related concerns (Meerow and Keith 2022). Studies find that planning and resource direction mirror this emphasis: managing acute heat events or mitigation of the Urban Heat

Island are repeatedly cited as priorities (Keith et al. 2019, Turner et al. 2022). While not all cities have access to shade data, those that do have integrated shade targets into heat-planning (City of Phoenix 2024, Los Angeles County 2026). Making more data available is not sufficient to guarantee its use (Findlater et al. 2021); however, in the case of shade, a whole class of data is missing from practitioners' heat-related decision-set. This study draws from data developed for the American Forests Tree Equity Score, a widely used and free, online user-oriented decision support tool (American Forests 2026). Making shade data more widely available and usable to cities through standard geospatial products is, therefore, a critical step in expanding access.

Our study has some key limitations for fully integrating shade data into land systems models and local practitioner decisions. Foremost, our data is aggregated at the census block scale, while shade varies at hyper-local scales, as do its benefits, including reducing radiant heat exposure. Future research should examine if and how higher resolution data sets augment the dynamics related to urban form and climate examined in this study. Additionally, modeled shade is not a direct analog to experienced heat burden. Shade coverage reflects the interruption of direct solar radiation, a key but partial determinant of heat burden that operates alongside air temperature, humidity, and individual physiology. Linking shade patterns to relevant metrics such as MRT or physiological outcomes will strengthen understanding of the public health benefits derived from them and forge stronger links to particular heat exposure settings (e.g., home, labor, school) and their governance (Ahmed et al., 2026). Of particular importance to cities may be deriving place-specific shade targets based on realistic floor-to-ceiling parameters, as well as reductions in metabolic work based on how space is used. The relationship between shade distribution and social vulnerability also warrants dedicated analysis; the diurnal role of building shade in densely populated, less-vegetated urban areas complicates straightforward interpretation and merits its own investigation (Gu et al., 2026). While this research establishes regional climate as a more dominant driver of shade abundance than the local urban climate, it does not consider key underlying factors. We do not examine how regional underlying variables such as precipitation and growing season lengths, or local variables such as building heights and impervious surface fractions influence shade availability. Future research should investigate these underlying mechanisms within regional and local climate zones to better understand how they drive shade abundance.

Finally, our study examines patterns based on a diurnal cross-section of one summer day from different years because of data constraints.This research was limited to using the best available open LiDAR dataset available for each city. A true panel data set of patterns over time would enable causal analysis of key drivers of change, including planning and policy interventions in urban form and forestry, as well as climate change impacts.

4. Materials and Methods

4.1 Surface modeling

Accurate representation of the physical urban space is critical to mapping shade distribution. We utilized highly detailed LiDAR point cloud data from the United States Geological Survey (USGS) 3D Elevation Program. The data is hosted on an Amazon Web Services server in Entwine Point tiles format. We developed a Python-based workflow to send getRequests to the server and fetch points intersecting each city's limits, which we obtained from America Forests. The workflow generates three (3) surface models on-the-fly after filtering points classified as noise and writes them to a file. These surface models are a full digital surface model (FDSM), which captures the height of all features above the earth's surface and the ground. The other two surface models are a Digital Elevation Model-DEM (ground points only) and a Full canopy height model- FCHM (the above-ground height of all features). We develop the final input surface models for SOLWEIG in a quality control process that follows this step.

We provide a table summarizing the acquisition dates for the point cloud as a supplementary material to this work.

SOLWEIG requires 2 surface models: a surface model of buildings and ground alone (BSM), and a vegetation canopy model (CDSM) to estimate the shadows from trees and buildings at a given time. We followed the approach of (Buo et al., 2023) to generate BSM by masking the FDSM with building footprints from the Microsoft building database and filling areas outside the buildings with their respective pixel values in the DEM. We performed a reverse masking operation on the FCHM using the building footprints to get vegetation canopies only and set areas covered by buildings to zero (0). In addition, we set the pixel values less than 1.3 m in the CDSM to zero because we do not consider them high enough to provide shading for the average person when standing.

4.2 Shade modeling

We determined the shade provided by buildings and trees using the shadowing function in SOLWEIG, applying a transmissivity value of 3% (Eq. 1). We generated the shadows for the summer solstice of 2023 (21/06/2023) at three key timestamps (12:00, 15:00, and 18:00 h) of the day to get a general progression of shading during the day. All simulations reflect conditions at local times for all cities while accounting for their time zones. The summer solstice and these specific times guarantee that the sun will be above the horizon in all cities while ensuring conditions at solar noon are captured.

Each city had 9 sets of rasters, vegetation, buildings, and total shade for the different timestamps. Simulating shadows with SOLWEIG is an iterative process in which a surface model continuously shifts, reducing its height at each step according to the solar altitude to determine the shadow volume (Lindberg & Grimmond, 2011). SOLWEIG resolves the total shade for a pixel by accounting for building and vegetation shade in the equation below (Lindberg & Grimmond, 2011).

$$Sh_i = Sh_{building} - (1 - Sh_{canopy}) * (1 - \tau) \quad (1)$$

where Sh_i indicate, $Sh_{building}$ indicates shade from building, Sh_{canopy}indicates shade from trees, and τ indicates transmissivity.

4.3 Shade scoring and disparity

We aimed to calculate a single score for each shade type and the CBG scale for each city. We determined the total outdoor space for each block group by performing an overlay operation using the building footprints and the boundaries of the CBGs. We proceeded to calculate the fraction of the total outdoor space covered by shade from buildings and vegetation at the selected times of the day. We also determined the percentage of total shade. Each census block group had a shade coverage score for total, building, and vegetation shade at 12:00, 15:00, and 18:00 h. We further determined the evenness of shading quality across the block groups in each city by calculating a Gini index for each city at these times.

4.4 Evaluating urban form, climate zone, and shade distribution

We investigated the effect of climate and urban form on the distribution of shade cities. We employed the Köppen-Geiger (KPG) climate classification system to evaluate the effects of climate on the shading quality. The KPG system groups regions into 5 main groups with 30 subgroups based on temperature and seasonal precipitation patterns (Beck et al., 2018; Köppen, 1936). We used the Local Climate Zone (LCZ) classification proposed by Stewart & Oke (2012), which categorizes urban areas according to the geometric configuration of features and land cover types. The LCZ scheme has six (6) and ten (10) classes governed by landcover properties and geometric configurations, respectively (Oke et al., 2017; Stewart & Oke, 2012). We used the version produced for the United States by (Bechtel et al., 2019). We analyzed the distribution of shade types across climate categories. We further investigated how both classifications affect the shading quality of a city and their significance using a Type I two-way ANOVA analysis. In the ANOVA analysis, we set KPG as the main effect variable to account for underlying environmental variables, latitudinal variations in solar angles, and vegetation types.

Declarations

Funding

This work was supported by the Robert Wood Johnson Foundation (grant no. 20235061 to V.K.T.)

Author Contributions

All authors conceived and designed the study. V.K.T led study design, analysis, and drafting. I.B. generated the data set, performed the analysis, and contributed to drafting. A.M. contributed to study design, analysis, and drafting. J.C.I contributed to analysis and drafting. All authors reviewed and edited the manuscript and approved the final version.

Data Availability

The derived shade datasets generated in this study are available from the corresponding author (V.K.T.) upon reasonable request.

References

1. J. Vanos *et al.*, A physiological approach for assessing human survivability and liveability to heat in a changing climate. *Nature communications* 14, 7653 (2023).
2. O. Jay *et al.*, Reducing the health effects of hot weather and heat extremes: from personal cooling strategies to green cities. *The Lancet* 398, 709–724 (2021).
3. J. Vanos *et al.*, A physiological approach for assessing human survivability and liveability to heat in a changing climate. *Nature Communications* 14 (2023).
4. I. D. Stewart, T. R. Oke, Local Climate Zones for Urban Temperature Studies. *Bulletin of the American Meteorological Society* 93, 1879–1900 (2012).
5. A. Martilli, E. S. Krayenhoff, N. Nazarian, Is the Urban Heat Island intensity relevant for heat mitigation studies? *Urban Clim* 31, 100541 (2020).
6. A. Middel, E. S. Krayenhoff, Micrometeorological determinants of pedestrian thermal exposure during record-breaking heat in Tempe, Arizona: Introducing the MaRTy observational platform. *Sci Total Environ* 687, 137–151 (2019).
7. F. A. Schneider, E. Epel, A. Middel, A disconnect in science and practitioner perspectives on heat mitigation. *npj Urban Sustainability* 4 (2024).
8. S. R. AlKhaled, A. Middel, P. Shaeri, I. Buo, F. A. Schneider, WebMRT: An online tool to predict summertime mean radiant temperature using machine learning. *Sustain Cities Soc* 115, 105861 (2024).
9. N. H. Wong, C. L. Tan, D. D. Kolokotsa, H. Takebayashi, Greenery as a mitigation and adaptation strategy to urban heat. *Nature Reviews Earth & Environment* 2, 166–181 (2021).
10. A. Middel, S. Alkhaled, F. A. Schneider, B. Hagen, P. Coseo, 50 Grades of Shade. *Bulletin of the American Meteorological Society* 102, E1805–E1820 (2021).
11. V. K. Turner, A. Middel, J. K. Vanos, Shade is an essential solution for hotter cities. *Nature* 619, 694–697 (2023).
12. A. Middel, K. Häb, A. J. Brazel, C. A. Martin, S. Guhathakurta, Impact of urban form and design on mid-afternoon microclimate in Phoenix Local Climate Zones. *Landscape Urban Plan* 122, 16–28 (2014).
13. B. Chen *et al.*, Advancing urban shade mapping for planning: Integrating shade demand and greening potential. *Urban for Urban Gree* 111, 128888 (2025).
14. W. Zhou, G. Huang, A. Troy, M. L. Cadenasso, Object-based land cover classification of shaded areas in high spatial resolution imagery of urban areas: A comparison study. *Remote Sens Environ* 113,

1769–1777 (2009).

15. O. Aleksandrowicz, "Chapter 1 - Mapping and management of urban shade assets: a novel approach for promoting climatic urban action" in Global Urban Heat Island Mitigation, A. Khan, H. Akbari, F. Fiorito, S. Mithun, D. Niyogi, Eds. (Elsevier, 2022), https://doi.org/10.1016/B978-0-323-85539-6.00003-2, pp. 1–27.
16. I. Buo, V. Sagris, J. Jaagus, A. Middel, High-resolution thermal exposure and shade maps for cool corridor planning. *Sustain Cities Soc* 93, 104499 (2023).
17. C. T. J. Roebroek *et al.*, Potential tree cover under current and future climate scenarios. *Sci Data* 12 (2025).
18. C. R. Nitschke *et al.*, The influence of climate and drought on urban tree growth in southeast Australia and the implications for future growth under climate change. *Landscape Urban Plan* 167, 275–287 (2017).
19. M. C. Peel, B. L. Finlayson, T. A. Mcmahon, Updated world map of the Köppen-Geiger climate classification. *Hydrology and Earth System Sciences* 11, 1633–1644 (2007).
20. R. Saud, S. M. Richter, LiDAR-based shade mapping: Decomposition and multi-resolution analysis in a 3D digital twin. *Remote Sensing Applications: Society and Environment* 41, 101918 (2026).
21. J. Dong, G. Metternicht, P. Hostert, R. Fensholt, R. R. Chowdhury, Remote sensing and geospatial technologies in support of a normative land system science: status and prospects. *Current Opinion in Environmental Sustainability* 38, 44–52 (2019).
22. V. Kelly Turner *et al.*, More than surface temperature: mitigating thermal exposure in hyper-local land system. *Journal of Land Use Science* 17, 79–99 (2022).
23. L. Li *et al.*, Divergent urbanization-induced impacts on global surface urban heat island trends since 1980s. *Remote Sens Environ* 295, 113650 (2023).
24. A. Middel, N. Selover, B. Hagen, N. Chhetri, Impact of shade on outdoor thermal comfort—a seasonal field study in Tempe, Arizona. *International Journal of Biometeorology* 60, 1849–1861 (2016).
25. S. Meerow, L. Keith, Planning for Extreme Heat. *Journal of the American Planning Association* 88, 319–334 (2022).
26. L. Keith, S. Meerow, T. Wagner, Planning for Extreme Heat: A Review. *Journal of Extreme Events* 06, 2050003 (2019).
27. C. o. Phoenix (2024) Shade Phoenix: An action plan for Trees and Build shade. (City of Phoenix).
28. L. A. County (2026) Los Angeles County Heat Action Plan. (Los Angeles County Chief Sustainability Office).
29. K. Findlater, S. Webber, M. Kandlikar, S. Donner, Climate services promise better decisions but mainly focus on better data. *Nature Climate Change* 11, 731–737 (2021).
30. A. Forest (2025) Tree Equity Score.
31. F. Lindberg, C. S. B. Grimmond, The influence of vegetation and building morphology on shadow patterns and mean radiant temperatures in urban areas: model development and evaluation.

Theoretical and applied climatology 105, 311–323 (2011).

32. H. E. Beck *et al.*, Present and future Köppen-Geiger climate classification maps at 1-km resolution. *Sci Data* 5, 180214 (2018).
33. W. Koppen, Das geographische system de klimate. *Handbuch der klimatologie* (1936).
34. T. R. Oke, G. Mills, A. Christen, J. A. Voogt, *Urban climates* (Cambridge university press, 2017).
35. B. Bechtel *et al.*, SUHI analysis using Local Climate Zones—A comparison of 50 cities. *Urban Clim* 28, 100451 (2019).

Figures

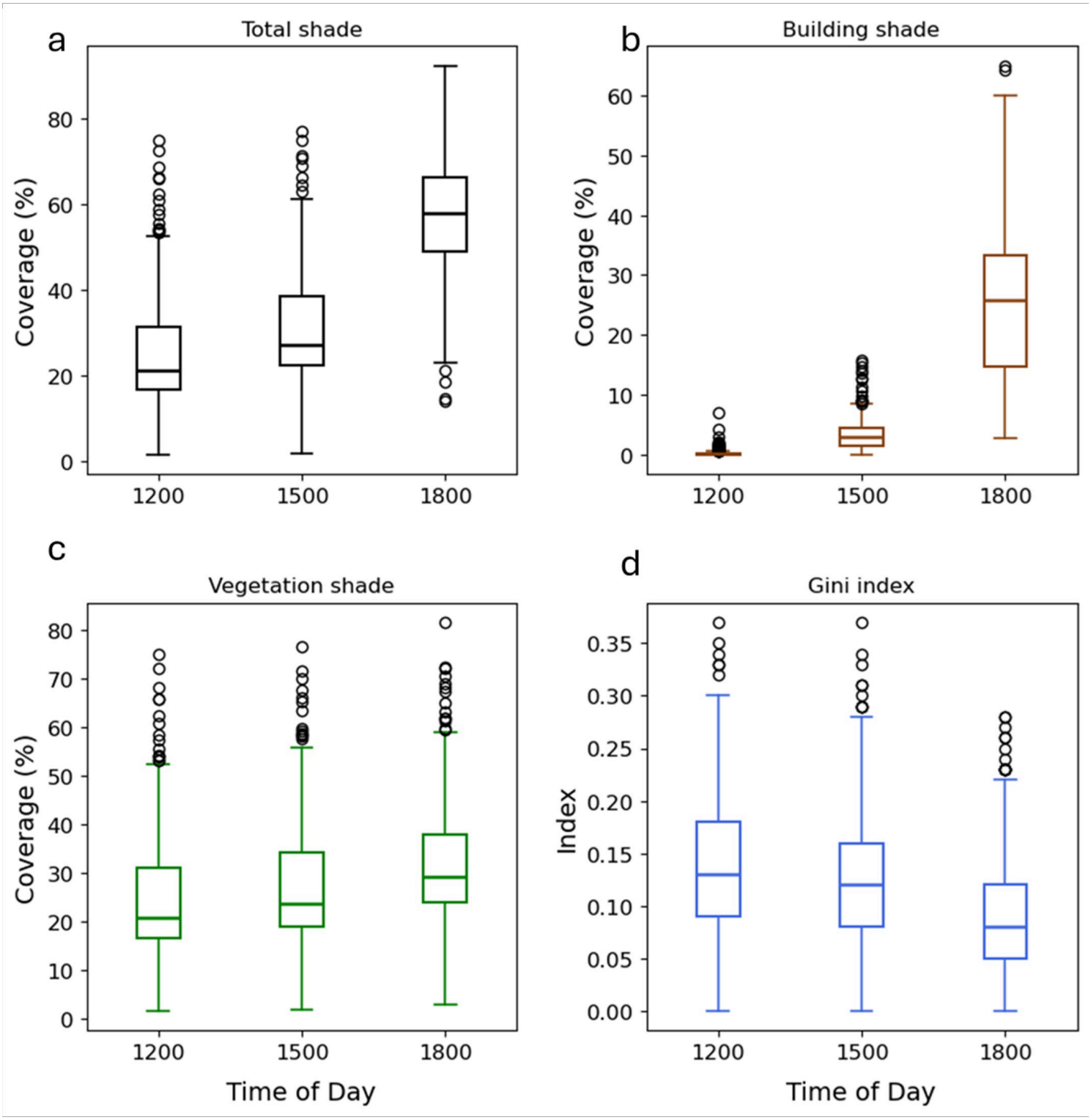


Figure 1

Summary of shade characteristics across CBGs in 330 U.S. Cities at 12:00, 15:00, and 18:00 h, including (a) total shade, (b) building shade, (c) vegetation shade, and (d) Gini index as a measure of disparity in total shade between CBGs within cities.

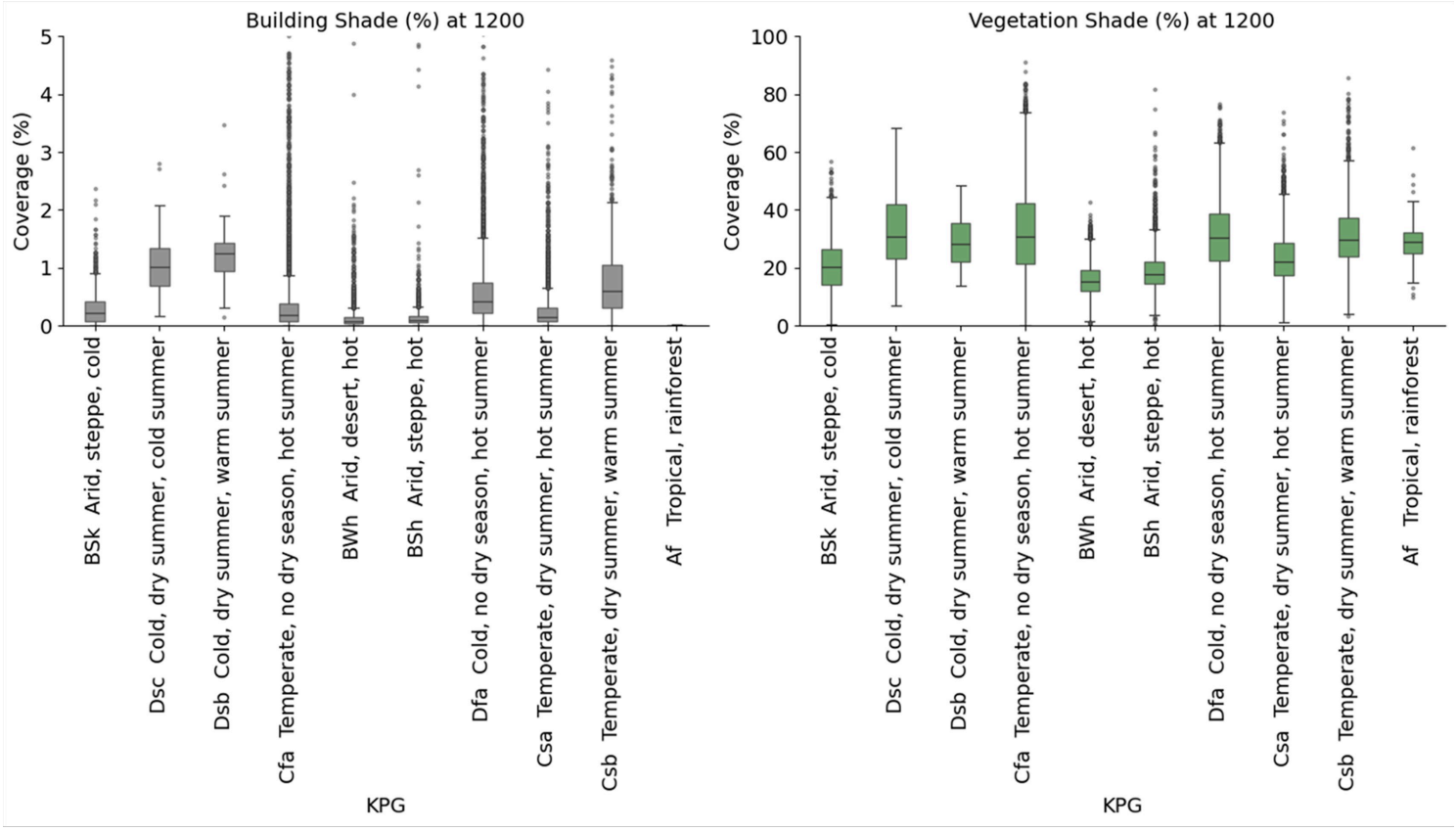


Figure 2

Percent building and vegetation shade by Köppen climate classification (KPG) at 12:00 h.

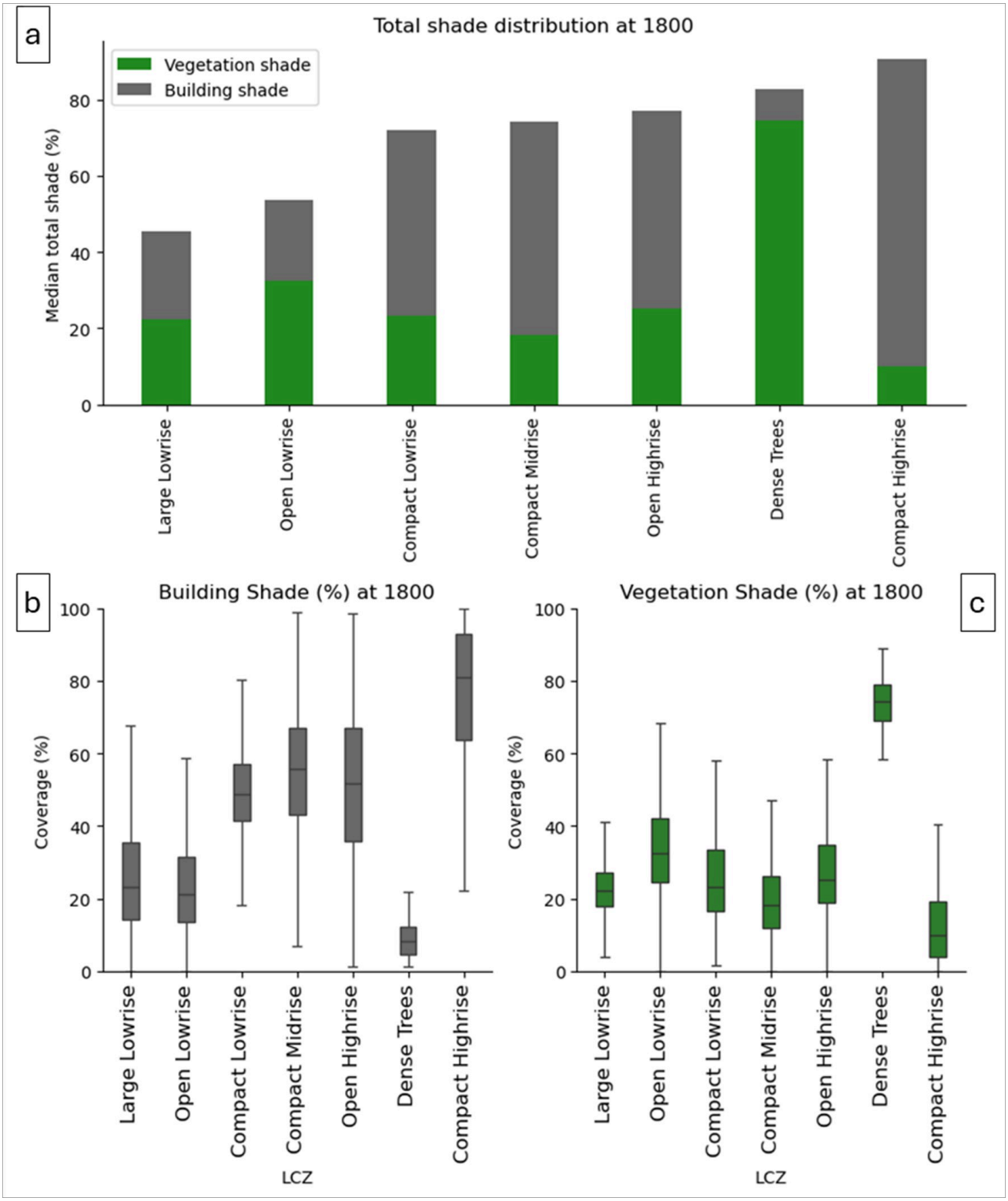


Figure 3

Percent total, building, and vegetation shade by Local Climate Zone (LCZ) at 18:00 h.

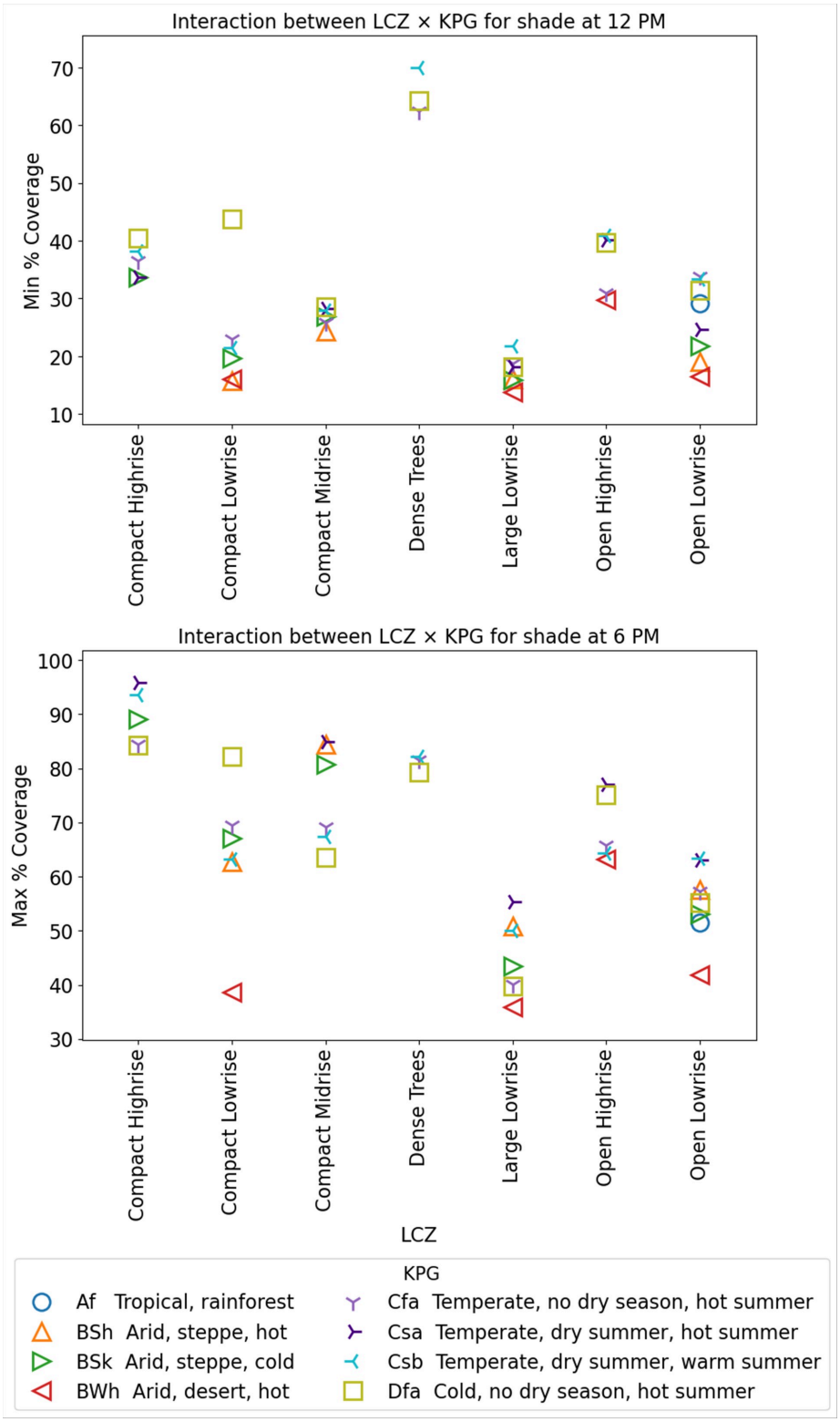


Figure 4

Interaction between Local Climate Zones (LCZ) and Köppen climate classification (KPG) at 12:00 h (minimum shade coverage) and 18:00 h (maximum shade coverage).

Supplementary Files

This is a list of supplementary files associated with this preprint. Click to download.

- Turneretal.NatureCitiesSubmissionappendices.docx